S-matrix analysis of heavy-ion elastic scattering

V. Chisté, R. Lichtenthäler, A. C. C. Villari,* and L. C. Gomes
Departamento de Física Nuclear, Laboratório do Pelletron, Instituto de Física, Universidade de São Paulo, Caixa Postal 66318, 05389-970 - São Paulo, SP, Brasil
(Received 25 October 1995)

A procedure to minimize χ^2 is described which explores the fact that the χ^2 distribution is of the fourth degree in the *S*-matrix elements. The fact that all three roots of the scale parameter for the minimum of χ^2 in its gradient direction are algebraically determined gives the present procedure some global features that previous methods did not contemplate. The automatic search procedure also preserves the unitary bound constraint of the *S*-matrix at every step. When the search in the gradient direction slows down, the procedure reverts to the traditional quadratic approximation with zero-order regularization. The method is applied to the elastic scattering of the $^{12}C+^{16}O$ reaction near the Coulomb barrier. [S0556-2813(96)02008-0]

PACS number(s): 24.10.−i, 25.70.Bc

I. INTRODUCTION

The analysis of the elastic scattering channel of heavy-ion collisions near the Coulomb barrier has been extensively done with the help of the Woods-Saxon (WS) optical potential [1]. Much of what we learned came from these analyses which give a somewhat structure less behavior of the collision. Another approach to the analysis of these collisions, the algebraic potential based on the SO(3,1) symmetry, has been proposed by Alhassid and Iachello [2]. In actual applications, this approach showed properties similar to the WS potential [3,4] and, at this moment, it is not clear whether the algebraic approach has a physical content different from the WS optical potential. However, extensive measurements and analysis of light heavy-ion systems [5–9] have shown resonances that cannot be easily explained in the context of the WS optical potential. These resonances of total widths of the order of 300 keV preclude such a simple explanation and suggest that a rich intermediate structure is present in the collision.

An alternative way out of this scheme, at least for spinless collisions, is to use *S*-matrix or phase shift analysis. Even in this case, a systematic study of the intermediate structure was made difficult by the lack of a reliable automatic, stable search for the *S*-matrix elements for the elastic channel. It is the absence of stability that made unreliable the phase shift analysis in heavy-ion collisions. Very frequently, starting the search from different initial conditions, different sets for the *S* matrix were found which had different physical contents.

In this paper, we present a procedure for determining the *S*-matrix elements for spinless collisions, which converges automatically to a physical solution even when 25 angular momentum channels are simultaneously searched. The procedure is based on the simple observation that the χ^2 function for the angular distribution is a fourth degree polynomial in the *S*-matrix elements. In contrast, the procedure of Krappe and Rossner [10] considers the highly nonlinear transformation $S_\ell = \exp(\eta_{\ell 1} + i\,\eta_{\ell 2}^2)$. The present procedure turns out to be stable when analyzing, without external manipulation, 16 elastic angular distributions of the $^{12}C+^{16}O$ system.

II. THE PROCEDURE

We write the scattering amplitude as

$$f(\theta) = f_c(\theta) + f_n(\theta),$$

where

$$f_c(\theta) = -\eta\, \exp(2i\sigma_0) \frac{\exp[-i\eta\, \ln\sin^2(\theta/2)]}{2k\, \sin^2(\theta/2)}$$

is the Coulomb amplitude and

$$f_n(\theta) = \frac{1}{2ik} \sum_{\ell=0}^{\infty} (2\ell+1) S_\ell^c (S_\ell^n - 1) P_\ell(\cos\theta) \qquad (1)$$

is the nuclear part of the total amplitude. The purpose of the procedure is to search for the unknown matrix elements S_ℓ^n, from $\ell = 0$ up to $\ell = \ell_{\max}$ which minimize the χ^2 defined by

$$\chi^2 = \sum_{j=1}^{N} \frac{[\sigma(\theta_j) - \sigma^e(\theta_j)]^2}{\Delta^2(\theta_j)},$$

where $\sigma^e(\theta_j)$ are the experimental cross sections and $\Delta(\theta_j)$ the experimental errors at the center of mass angle θ_j. The search proceeds first in the direction of the gradient in the parameter space. The choice of $\ell_{\max}$ depends on the size of the system and the energy under consideration, and for angular momenta ℓ above this value the *S*-matrix elements are assumed to be unity. We write $S_\ell^n = x_\ell + iy_\ell$ and set

*Present Address: GANIL. B. P. 5027, 14021-Caen, Cedex, France.

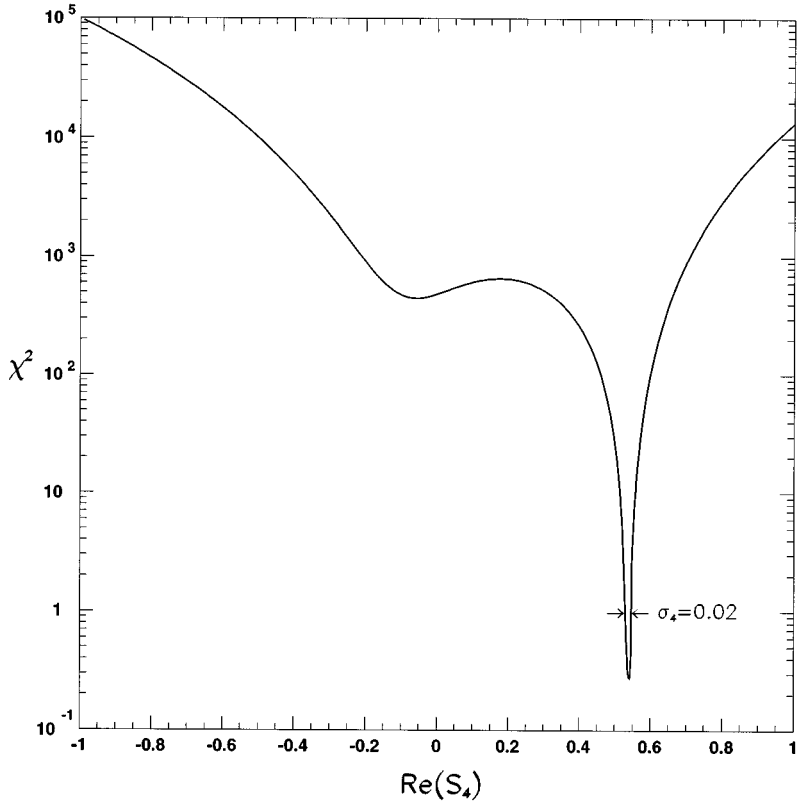

FIG. 1. χ^2 as function of Re(S_4) for a simulated case. It also exhibits σ_4, the estimated error for Re(S_4).

$$u_\ell = \frac{\partial \chi^2}{\partial x_\ell}$$

$$= \frac{2(2\ell+1)}{k} \sum_{j=1}^{N} \frac{\sigma(\theta_j) - \sigma^e(\theta_j)}{\Delta^2(\theta_j)} P_\ell(\cos\theta_j) \mathrm{Im}[f^*(\theta_j) S_\ell^c],$$

$$v_\ell = \frac{\partial \chi^2}{\partial y_\ell} = \frac{2(2\ell+1)}{k} \sum_{j=1}^{N} \frac{\sigma(\theta_j) - \sigma^e(\theta_j)}{\Delta^2(\theta_j)}$$

$$\times P_\ell(\cos\theta_j)\ \mathrm{Re}[f^*(\theta_j) S_\ell^{(c)}].$$

We write

$$S_\ell^n = S_\ell'^n + \alpha(u_\ell + i v_\ell), \tag{2}$$

where $S_\ell'^n$ is the previous and S_ℓ^n the new matrix element shifted in the direction of the gradient of χ^2.

Substituting the previous equation in the expression for χ^2 we obtain a polynomial of the fourth degree in the scale factor α:

$$\chi^2 = A\alpha^4 + B\alpha^3 + C\alpha^2 + D\alpha + \chi_0^2,$$

where the coefficients A, B, C, and D are easily obtained in analytical form. We set

$$\phi(\theta) = \frac{1}{2ik} \sum_{\ell \in L} (2\ell+1) S_\ell^c (u_\ell + i v_\ell) P_\ell(\cos\theta),$$

and we have

$$A = \sum_{j=1}^{N} \frac{|\phi(\theta_j)|^4}{\Delta^2(\theta_j)}, \tag{3}$$

$$B = 4 \sum_{j=1}^{N} \frac{|\phi(\theta_j)|^2}{\Delta^2(\theta_j)} \mathrm{Re}[f(\theta_j)\phi^*(\theta_j)], \tag{4}$$

$$C = 2 \sum_{j=1}^{N} \frac{|\phi(\theta_j)|^2}{\Delta^2(\theta_j)} [\sigma(\theta_j) - \sigma^e(\theta_j)]$$

$$+ 4 \sum_{j=1}^{N} \frac{\{\mathrm{Re}[f(\theta_j)\phi^*(\theta_j)]\}^2}{\Delta^2(\theta_j)}, \tag{5}$$

$$D = \sum_{\ell=\ell_{\min}}^{\ell_{\max}} (u_\ell^2 + v_\ell^2). \tag{6}$$

The values of α for which χ^2 is an extremum are given by the roots of the cubic equation:

$$4A\alpha^3 + 3B\alpha^2 + 2C\alpha + D = 0. \tag{7}$$

The values of A and D are positive which indicates that the cubic equation always has at least one negative root which corresponds to the local minimum in the negative direction of the gradient. Quite often the equation has three real roots indicating the existence of a second minimum. Our search procedure always considers the possibility of branching to this second minimum whenever the value of χ^2 at the minimum is smaller than the value at the local minimum. Figure 1 exhibits the value of χ^2 as a function of Re(S_ℓ) for $\ell = 4$ at a typical situation of the analysis of the $^{12}C + ^{16}O$ angular distribution. The experimental points were actually,

TABLE I. A summary of the 16 energies analyzed. The labels of the columns are explained in the text.

$E_{\text{c.m.}}$ (MeV)	$\ell_{\max}$	N_0	N	χ^2
8.549	9	42	22	20
9.064	9	43	23	13
10.010	12	43	17	14
11.040	13	43	15	12
11.980	13	44	16	16
13.013	14	41	11	13
14.042	15	45	13	14
14.984	16	44	10	41
17.280	19	87	47	50
19.400	19	68	28	5.8
20.790	20	87	45	34
21.860	21	88	44	19
23.140	23	103	55	5.5
24.490	24	84	34	3.5
25.500	24	88	38	10
26.740	25	87	35	4.9

in this case, simulated by an optical potential. The errors in the equation for χ^2 were assumed constant and equal to 10%. One clearly observes, within the interval $[-1,1]$ for $\mathrm{Re}(S_4)$, the presence of two minima for χ^2. This simple case illustrates that a search based only in the local gradient direction, depending on where the search starts, finds the false minimum. In our procedure, for the case illustrated, it finds the true minimum in a single iteration. In this figure we also have shown the estimated error $\sigma_4=0.02$ for $\mathrm{Re}(S_4)$ as the width of curve calculated where χ^2 is one unit above its minimum value.

Before making the choice at which minimum to branch to, we impose the unitary bound for each S_ℓ.

The equation $|S'^n_\ell+\alpha(u_\ell+iv_\ell)|=1$ gives

$$\alpha^2(u_\ell^2+v_\ell^2)+2\gamma_\ell\alpha-(1-|S'^n_\ell|^2)=0 \tag{8}$$

with $\gamma_\ell=u_\ell x'_\ell+v_\ell y'_\ell$. The two roots of this equation are

$$\alpha'_\ell=-\frac{\gamma_\ell+\sqrt{\gamma_\ell^2+(u_\ell^2+v_\ell^2)(1-|S'^n_\ell|^2)}}{u_\ell^2+v_\ell^2}\leqslant 0,$$

$$\alpha''_\ell=-\frac{\gamma_\ell-\sqrt{\gamma_\ell^2+(u_\ell^2+v_\ell^2)(1-|S'^n_\ell|^2)}}{u_\ell^2+v_\ell^2}\geqslant 0.$$

The unitary bound on each S_ℓ is easily imposed by writing the new values as $S'^n_\ell+\alpha_\ell(u_\ell+iv_\ell)$ with

$$\begin{aligned}\alpha_\ell&=\alpha'_\ell \text{ for } \alpha_\ell<\alpha'_\ell\\ &=\alpha_\ell \text{ for } \alpha'_\ell\leqslant\alpha_\ell\leqslant\alpha''_\ell\\ &=\alpha''_\ell \text{ for } \alpha_\ell\geqslant\alpha''_\ell.\end{aligned}$$

The case when $\alpha'_\ell=\alpha''_\ell=0$ needs consideration. This occurs whenever the S_ℓ is on the unitary circle ($|S'_\ell|=1$) and the gradient is tangent to this circle ($\gamma_\ell=0$). In this particular case we write $S_\ell^{(n)}=S'_\ell\exp(i\beta_\ell)$ with $\beta_\ell=\alpha_0(v_\ell x'_\ell-u_\ell y'_\ell)$, which corresponds to a displacement on the unitary circle.

TABLE II. The parameters of the four Regge poles observed in the 23.14 MeV angular distribution.

ℓ_0	$\Gamma/2$	Δ
13.50	2.25	3.00
6.50	0.93	1.51
2.70	1.00	1.50
0.00	0.75	1.20

The search along the gradient directions stops whenever the value of the gradient is sufficiently small to guarantee that, in Eq. (7), the linear approximation is valid. When this happens, the procedure reverts to a search in every direction of the parameter space by changing the above method to the standard one [11] based on the quadratic approximation for χ^2. To avoid instability due to the large number of parameters involved, the zero-order regularization [12] was introduced.

III. THE QUADRATIC APPROXIMATION

We assume L to be the interval $[\ell_{\min},\ell_{\max}]$ and set $\ell_1=\ell_{\min}-1$ and $\ell_2=\ell_{\max}-\ell_{\min}+1$. Changing to the notation $a_i=x_{i+\ell_1}$ and $a_{i+\ell_2}=y_{i+\ell_1}$ we write

$$\chi^2=\chi_0^2+\sum_i B_i\Delta a_i+\frac{1}{2}\sum_{im}A_{im}\Delta a_i\Delta a_m$$

with

$$B_i=\frac{\partial\chi^2}{\partial a_i},$$

$$A_{im}=\frac{\partial^2\chi^2}{\partial a_i\partial a_m}.$$

The new values of the parameters are obtained shifting the old values by the following amount:

$$\Delta a_i=-\sum_m(A_{im}+\lambda\delta_{im})^{-1}B_m,$$

where λ is the regularizing parameter [12]. We set

$$\lambda=\frac{\mathrm{Tr}A}{2\ell_2},$$

and the search iterates until the variation of χ^2 between two successive iterations is less than 0.1%. At this point the errors δa_i and the correlation coefficients ρ_{im} are calculated by

$$\delta a_i=\sqrt{A_{ii}^{-1}},$$

$$\rho_{im}=\frac{A_{im}^{-1}}{\delta a_i\delta a_m}.$$

The analytical expressions for B_i and A_{im} are the following ($1\leqslant i,m\leqslant\ell_2$):

$$B_i=\frac{2}{k}[2(i+\ell_1)+1]\sum_j^N \frac{\sigma(\theta_j)-\sigma^e(\theta_j)}{\Delta^2(\theta_j)}P_{i+\ell_1}(\theta_j)\mathrm{Im}[(f^*(\theta_j)S^c_{i+\ell_1}],$$

$$B_{i+\ell_2}=\frac{2}{k}[2(i+\ell_1)+1]\sum_j^N \frac{\sigma(\theta_j)-\sigma^e(\theta_j)}{\Delta^2(\theta_j)}P_{i+\ell_1}(\theta_j)\mathrm{Re}[f^*(\theta_j)S^c_{i+\ell_1}],$$

$$A_{im}=\frac{1}{2k^2}[2(i+\ell_1)+1][2(m+\ell_1)+1]\sum_j^N \mathrm{Re}\left(\frac{2\sigma(\theta_j)-\sigma^e(\theta_j)}{\Delta^2(\theta_j)}S^c_{i+\ell_1}S^{c*}_{m+\ell_1}-\frac{f_j^{*2}}{\Delta^2(\theta_j)}S^c_{i+\ell_1}S^c_{m+\ell_1}\right)P_{i+\ell_1}(\theta_j)P_{m+\ell_1}(\theta_j),$$

$$A_{i+\ell_2,m+\ell_2}=\frac{1}{2k^2}[2(i+\ell_1)+1][2(m+\ell_1)+1]$$
$$\times\sum_j^N \mathrm{Re}\left(\frac{2\sigma(\theta_j)-\sigma^e(\theta_j)}{\Delta^2(\theta_j)}S^c_{i+\ell_1}S^{c*}_{m+\ell_1}+\frac{f_j^{*2}}{\Delta^2(\theta_j)}S^c_{i+\ell_1}S^c_{m+\ell_1}\right)P_{i+\ell_1}(\theta_j)P_{m+\ell_1}(\theta_j),$$

$$A_{i,m+\ell_2}=\frac{1}{2k^2}[2(i+\ell_1)+1][2(m+\ell_1)+1]$$
$$\times\sum_j^N \mathrm{Im}\left(\frac{2\sigma(\theta_j)-\sigma^e(\theta_j)}{\Delta^2(\theta_j)}S^c_{i+\ell_1}S^{c*}_{m+\ell_1}+\frac{f_j^{*2}}{\Delta^2(\theta_j)}S^c_{i+\ell_1}S^c_{m+\ell_1}\right)P_{i+\ell_1}(\theta_j)P_{m+\ell_1}(\theta_j),$$

$$A_{i+\ell_2,m}=\frac{1}{2k^2}[2(i+\ell_1)+1][2(m+\ell_1)+1]$$
$$\times\sum_j^N \mathrm{Im}\left(\frac{-2\sigma(\theta_j)+\sigma^e(\theta_j)}{\Delta^2(\theta_j)}S^c_{i+\ell_1}S^{c*}_{m+\ell_1}+\frac{f_j^{*2}}{\Delta^2(\theta_j)}S^c_{i+\ell_1}S^c_{m+\ell_1}\right)P_{i+\ell_1}(\theta_j)P_{m+\ell_1}(\theta_j).$$

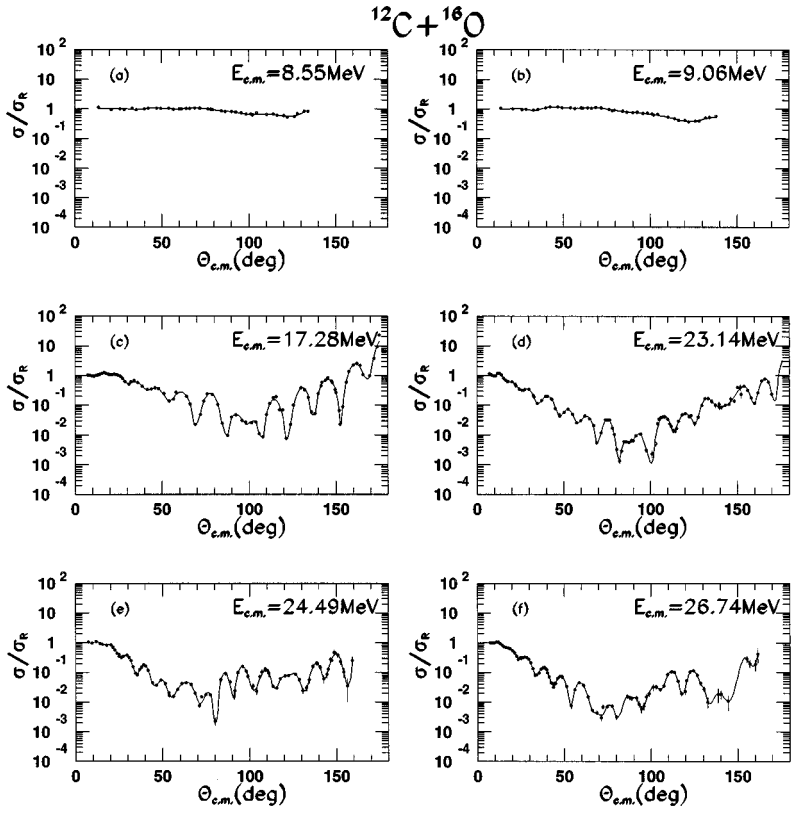

FIG. 2. The angular distribution fits for six analyzed energies.

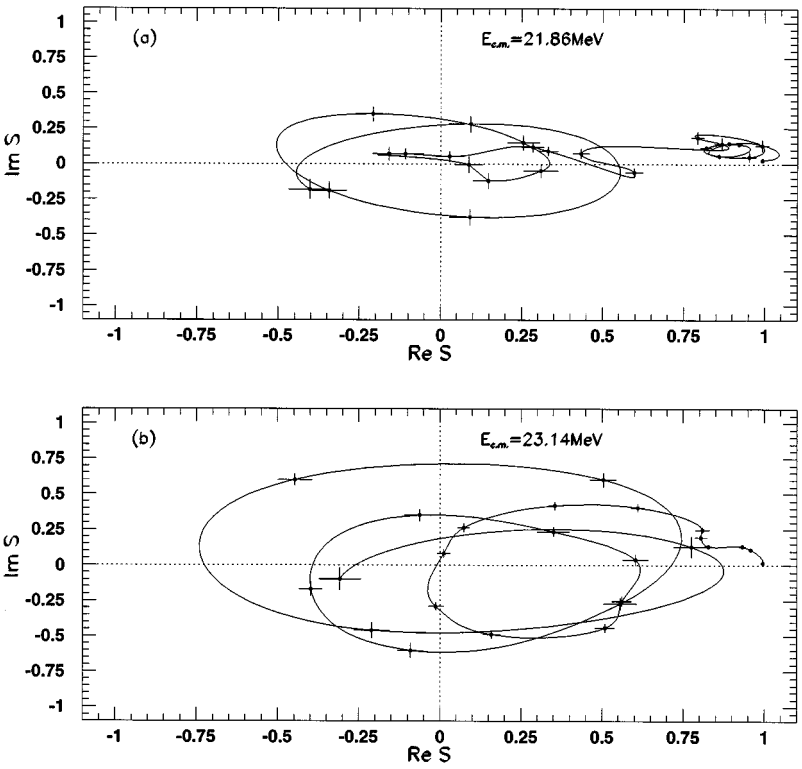

FIG. 3. The Argand diagrams for two consecutive analyzed energies as indicated. The solid lines are a guide to the eyes. The errors of the real and imaginary parts of the *S* matrix are indicated.

IV. THE $^{12}C+^{16}O$ ELASTIC CHANNEL

The procedure was applied to the analysis of 16 elastic angular distributions measured in the $^{12}C+^{16}O$ collision. The data were obtained by Fröhlich [8] in the range [8.549 MeV, 14.984 MeV], by Villari [13] (forward angles) and Charles [14] (backward angles) in the range [17.28 MeV, 21.86 MeV] and Villari [13] in the range [23.14 MeV, 26.74 MeV], with all energies referred to the center of mass sys-

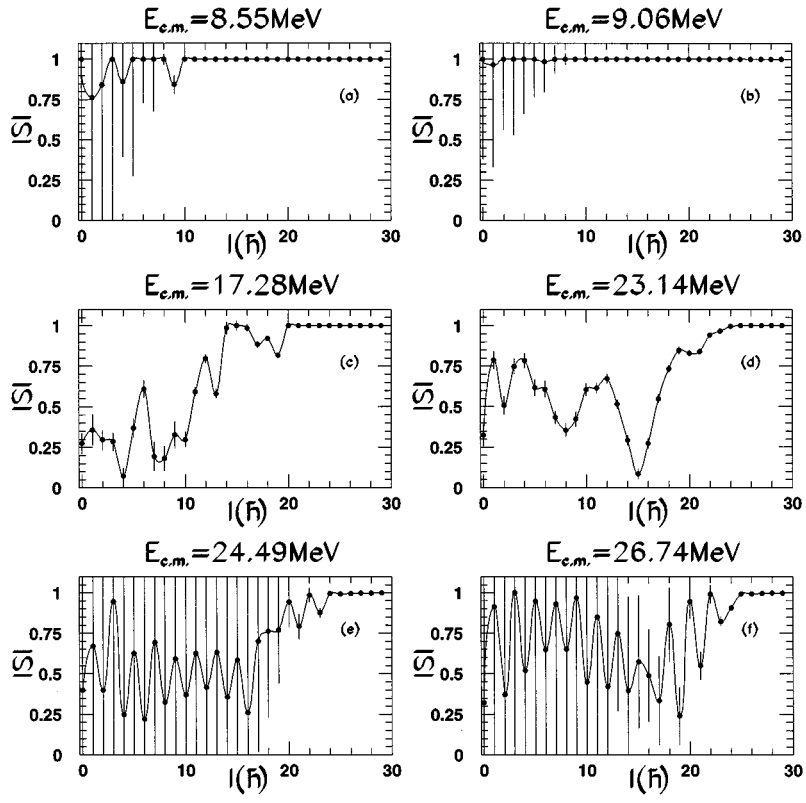

FIG. 4. The absolute value of the *S* matrix as a function of the angular momentum for six energies. The errors are indicated by the vertical bars.

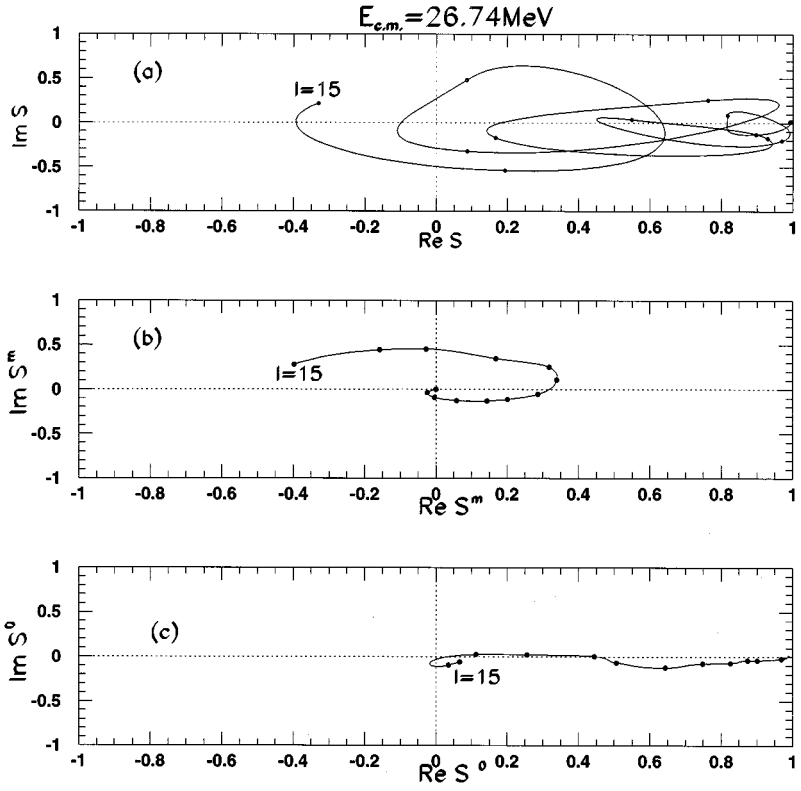

FIG. 5. The Argand diagrams for $15 \leqslant \ell \leqslant 30$ of (a) the total S matrix, (b) Majorana, and the (c) direct components of the S matrix for the energy indicated. The solid lines are a guide to the eyes.

tem. For each one of the analyzed distributions we started from an S matrix generated by the Woods-Saxon potential found by Charles [14], that describes mainly the forward diffractive part of the distributions.

Table I gives a summary of our results. The columns give the energy of the angular distribution in the center of mass system ($E_{\text{c.m.}}$), the maximum value of ℓ considered ($\ell_{\max}$), the number of experimental points measured (N_0), the number of degrees of freedom of the χ^2 distribution (N), and the reduced value of χ^2 after the analysis (χ^2/N). Once the initial set for the S matrix and the value of $\ell_{\max}$ were chosen, the search of the final solution proceeded without any intermediate manipulation. Figure 2 presents the fits obtained for six angular distributions at $E_{\text{c.m.}} = 8.55$, 9.06, 17.28, 23.14, 24.49, and 26.74 MeV. We observe that even in the worst case, at $E_{\text{c.m.}} = 17.28$ MeV with $\chi^2 = 50$, the fit is excellent. The apparently large value of χ^2 reflects the fact that we have included only the statistical errors ($< 1\%$), which underestimate the total errors of the measured cross sections [13]. The richness of structures in the angular distributions is reflected in the patterns observed in the Argand diagrams of the S matrix. A full discussion of all 16 distributions analyzed is beyond this paper but we consider here three features that were conspicuously seen.

Figure 3 exhibits two Argand diagrams for [Fig. 3(a)] 21.86 MeV and [Fig. 3(b)] 23.14 MeV as a function of the angular momentum, corresponding to two consecutive energies analyzed. The errors are also indicated in the figures. We observe that the errors decrease as ℓ increases as expected. Figure 3(b), in particular, exhibits a pattern of four loops around the origin which is the signature of the presence of four Regge poles [15]. The fact that the loops encircle the origin says that their partial widths are larger than half of the corresponding total widths, characterizing a strong coupling to the elastic channel [16]. The pole parameters were easily obtained from the S matrix and Table II gives the position (ℓ_0), the half total width ($\Gamma/2$) and the partial width (Δ) for each pole. Though the four poles are easily determined at 23.14 MeV, the neighboring distribution shows that at least one pole has moved drastically away from the origins of the diagrams making it difficult to follow the movements of the poles. This results because the energy intervals between the neighboring distributions are too large (> 1 MeV) in comparison to the widths of possible resonances in this energy region. The rapid variation of the diagrams, from one to the next neighboring energy, indicates that the structures are of intermediate character and not single-particle or potential resonances, whose widths are expected to be larger than 1 MeV. In any case, the presence of a few poles simultaneously at quite a few analyzed energies is a strong evidence of structures but of intermediate character. Such structures were already observed by Wilschut *et al.* [7]. Measuring angular distributions at steps less than 100 keV, from 19.50 MeV to 21.00 MeV in the c.m. system, these authors identified one resonance of total width equal to 300 ± 100 keV at 19.8 ± 0.1 MeV. At lower energies, Fröhlich *et al.* [8] were able to identify eight resonances between 8.5 MeV and 15 MeV, all of them with widths less than or equal to 320 keV.

In Fig. 4 the absolute value of S_ℓ is plotted as a function of ℓ at the same six energies as in Fig. 2. We observe that at $E_{\text{c.m.}} = 24.49$ and 26.74 MeV the errors are very large for low ℓ and that nothing can be concluded about the interaction. In spite of the large errors, the A matrix defined in Sec. III is not singular. The zigzag pattern of the points at

$E_{\text{c.m.}}=26.74$ MeV for $\ell \geq 15$ is a signature for the presence of an exchange component in the nuclear interaction, possibly due the exchange of α particles between target and projectile. Writing

$$S_\ell = S_\ell^0 + (-1)^\ell S_\ell^m ,$$

the direct (S_ℓ^0) and the Majorana (S_ℓ^m) components of the S matrix can easily be determined. Figures 5(b) and 5(c) exhibit this decomposition and we observe that the direct part of the interaction is purely absorptive while the Majorana component exhibits, possibly, one Regge pole. This clearly observed pattern could not be appreciated if we had plotted the two components together as it is shown in Fig. 5(a).

One question that is usually raised with respect to such searches is to what extent the set of values obtained for the S matrix is stable. To shed some light on this question we investigated the reason why some angular distributions yield small errors for the S matrix while others yield very large ones. Examining all 16 distributions we found that those resulting in large errors were precisely those that lacked experimental points for large angles ($\Theta_{\text{c.m.}} \geq 160°$). We conclude that the stability of the search strongly depends on the completeness of the angular distributions.

V. CONCLUSIONS

The procedure developed is able to search automatically the real and imaginary parts of the elastic S-matrix elements and its errors without violating the unitary bound. Sixteen angular distributions of the system $^{12}C + ^{16}O$ were analyzed and Regge poles and Majorana exchange components were identified in the S matrices.

We hope that the method presented will stimulate the measurements of the elastic channels for heavy-ion systems in a systematic way, especially in the region of importance for astrophysics, with small energy steps to map, all the possible mechanisms involved in a given energy resolution.

Partial support was provided by CAPES.

[1] G. R. Satchler, Phys. Rep. **199**, 147 (1991).
[2] Y. Alhassid and F. Iachello, Nucl. Phys. **A501**, 585 (1989).
[3] R. Lichtethäler and L. C. Gomes, Phys. Rev. C **50**, 3163 (1994).
[4] R. Lichtenthäler, D. Pereira, L. C. Chamon, L. C. Gomes, A. Ventura, and L. Zuffi, Phys. Rev. C **50**, 3033 (1994).
[5] E. Almqvist, D. A. Bromley, and F. A. Kuehner, Phys. Rev. Lett. **4**, 365 (1960).
[6] D. A. Bromley, F. A. Kuehner, and E. Almqvist, Phys. Rev. Lett. **4**, 515 (1960).
[7] H. W. Wilschut, P. Braun-Munzinger, G. M. Berkowitz, R. H. Freifelder, J. S. Karp, and T. R. Renner, Phys. Lett. **38**, 944 (1977).
[8] H. Fröhlich, P. Dück, W. Trev, and H. Voit, Phys. Rev. C **27**, 578 (1983).
[9] N. Cindro, Ann. Phys. (France) **13**, 289 (1983).
[10] H. J. Krappe and H. H. Rossner, Z. Phys. A **314**, 149 (1983).
[11] P. R. Bevington, *Data Reduction and Error Analysis for the Physical Sciences* (McGraw-Hill, New York, 1969).
[12] W. H. Press, S. A. Teukolsky, W. T. Vettering, and B. P. Flannery, *Numerical Recipes in C* (Cambridge University Press, Cambridge, England, 1992).
[13] A. C. C. Villari, A. Lépine-Szily, R. Lichtenthäler Filho, O. Portesan Filho, M. M. Obuti, J. M. Oliveira, Jr., and N. Added, Nucl. Phys. **A501**, 605 (1989).
[14] P. Charles, Ph.D. thesis, Orsay, France, 1981.
[15] V. de Alfaro and T. Regge, *Potential Scattering* (North-Holland, Amsterdam, 1965)
[16] K. M. McVoy, Phys. Rev. C **3**, 1104 (1971).